

## The NMR structure of protein-glutaminase from *Chryseobacterium proteolyticum*

Hiroyuki Kumeta · Noriko Miwa · Kenji Ogura ·  
Yuko Kai · Toshimi Mizukoshi · Nobuhisa Shimba ·  
Ei-ichiro Suzuki · Fuyuhiko Inagaki

Received: 16 December 2009 / Accepted: 9 February 2010 / Published online: 27 February 2010  
© Springer Science+Business Media B.V. 2010

### Biological context

Protein deamidation, the hydrolysis of side chain amido groups of protein-bound glutamyl or asparagyl residues to release ammonia, has received focused attention especially in food industries since protein deamidation is regarded as a promising method to improve functional properties of food proteins. Deamidation generally decreases an isoelectric point of proteins due to increase in number of negatively charged carboxyl groups and enhances protein solubility. In addition, deamidation leads to alteration of the tertiary structures of proteins with an improved amphiphilic character that is useful as an emulsifier or a foaming agent. Therefore, deamidation of food proteins have been investigated by various methods including mild acid treatment, anion-catalyzed deamidation, dry heating under mild alkaline conditions, and thermal treatment. Although deamidation by these treatments improved protein functionalities, there were undesired side-effects, such as concomitant peptide bond cleavages, that were unavoidably brought about by the chemical/physical treatments. Therefore, enzymatic methods have advantages due to their selectivity and mild treatments. The possibilities of the use of transglutaminases, peptidoglutaminases, and proteases have been explored for this purpose. These enzymes, however, are not suitable because the

primary catalytic reactions of transglutaminases and proteases are not deamidation itself, and primary substrates of peptidoglutaminases are not proteins.

Protein-glutaminase (PG) is an enzyme produced from the microorganism *Chryseobacterium proteolyticum* strain 9670 (Yamaguchi et al. 2001). PG catalyzes only the deamidation of the side chain amido group of protein-bound glutamyl residues to release ammonia without catalyzing the transglutamination and hydrolysis of asparagyl residues or producing other undesirable changes in protein structures. PG is a monomeric single polypeptide with pI = 10.0 and a molecular weight of 19,860 and is synthesized as a prepro-form, containing a 21-amino-acid signal polypeptide, a 114-amino acid pro-region, and a sequence for the mature enzyme. PG with the pro-region (pro-PG) has no enzymatic activities, but when pro-PG is removed by an extracellular protease, an active enzyme is produced in *C. proteolyticum*. However, the amount of PG produced by *C. proteolyticum* is too small to be used for industrial application that limits the application of PG to deamidation of food proteins.

Recently, we have constructed the high expression system of PG with *Corynebacterium glutamicum*, which enables us to prepare an amount of stable-isotope labeled PG for NMR experiments (Kikuchi et al. 2009). Here, we report the solution structure of mature PG determined by NMR and discuss the catalytic mechanism of PG on the structural basis.

H. Kumeta · K. Ogura · F. Inagaki (✉)  
Laboratory of Structural Biology, Graduate School  
of Pharmaceutical Sciences, Hokkaido University,  
Kita 12 Nishi 6, Kita-ku, Sapporo 060-0812, Japan  
e-mail: finagaki@pharm.hokudai.ac.jp

N. Miwa · Y. Kai · T. Mizukoshi · N. Shimba · E. Suzuki  
Institute of Life Sciences, Ajinomoto Co., Inc., 1-1 Suzuki-cho,  
Kawasaki-ku, Kawasaki-shi 210-8681, Japan

### Materials and methods

#### NMR spectroscopy

$^{15}\text{N}$  and  $^{13}\text{C}/^{15}\text{N}$  labeled PG were expressed and purified as described previously (Shinagawa et al. 2005). A suite of

two- and three-dimensional NMR experiments was performed on Varian UNITY inova spectrometers operating at 800 and 600 MHz at 25°C. Spectra were processed using NMRPipe (Delaglio et al. 1995) and data analysis was performed with the help of the Sparky program (Goddard and Kneller 1997).  $^1\text{H}$ ,  $^{13}\text{C}$  and  $^{15}\text{N}$  resonance assignments were carried out using the following set of spectra;  $^1\text{H}$ - $^{15}\text{N}$  HSQC,  $^1\text{H}$ - $^{13}\text{C}$  HSQC, HN(CO)CA, HNCA, CBCA(CO)NH, HNCACB, HNCO, HBHA(CO)NH, HN(CA)HA, HC(C)H-TOCSY, (H)CCH-TOCSY, HbCbCgCdHd, and HbCbCgCdCeHe. Interproton distance restraints were obtained using  $^{15}\text{N}$ -edited and  $^{13}\text{C}$ -edited NOESY-HSQC spectra using a 75 ms mixing time. Dihedral angle restraints were obtained from the chemical shift values using the TALOS program (Cornilescu et al. 1999).

### Structural calculation

The structure was calculated using the CYANA 2.1 software package (Herrmann et al. 2002). As an input for the final calculation of the three-dimensional structure of PG, a total of 4,252 distance and 232 angle restraints were used (Table 1). At each stage, 100 structures were calculated using 30,000 steps of simulated annealing, and a final ensemble of 20 structures was selected based on CYANA target function values. The atomic coordinates have been deposited in the Protein Data Bank (PDB code: 2KSV).

## Results and discussion

$^1\text{H}$ - $^{15}\text{N}$  HSQC spectrum of PG was well-dispersed as shown in Fig. 1A. Almost all of the resonances were

**Table 1** Structural statistics of the PG

NOE distance constraints	4,252
Short range (intraresidue and sequential)	2,109
Medium range ( $2 \leq  i - j  \leq 4$ )	716
Long range ( $ i - j  > 4$ )	1,427
Number of violations	
Distance $>0.3 \text{ \AA}$	1
Angle $>5^\circ$	0
Structural coordinates rmsd ( $\text{\AA}$ ) (range 141–315)	
Backbone atoms	0.34
All heavy atoms	0.59
Ramachandran plot	
Most favored regions	77.3%
Additionally allowed regions	22.1%
Generously allowed regions	0.6%
Disallowed regions	0%

assigned using a suite of conventional NMR spectra. The structure of PG was calculated using the CYANA 2.1 software package (Herrmann et al. 2002) based on the interproton distance restraints and dihedral angle restraints. The overlay of the 20 structures and the ribbon model of the lowest energy structure are shown in Fig. 1B, C. The PG formed a single, compact domain which comprises a large curved  $\beta$ -sheet ( $\beta 1$ ; 197–207,  $\beta 2$ ; 211–226,  $\beta 3$ ; 233–237,  $\beta 4$ ; 246–248,  $\beta 5$ ; 265–272), a small  $\beta$ -sheet ( $\beta 6$ ; 277–280,  $\beta 7$ ; 284–287), and four  $\alpha$ -helices ( $\alpha 1$ ; 143–156,  $\alpha 2$ ; 177–191,  $\alpha 3$ ; 250–256,  $\alpha 4$ ; 292–301). The three  $\alpha$ -helices ( $\alpha 1$ ,  $\alpha 2$  and  $\alpha 4$ ) and the small  $\beta$ -sheet were located on one side of the large curved  $\beta$ -sheet, while  $\alpha 3$  was located on the opposite side. An initial structural similarity search, performed with the calculated coordinates of PG using the DALI server (Holm et al. 2008), showed that PG has moderate structural similarity to the catalytic core domain of TGs (human TGase3; 1L9N, factor XIII; 1GGY and 1GGT, fish TGase; 1G0D), thiol proteinase-like domain of *Pasteurella multacida* toxin (2EBH) and mushroom lectin (2IHO) with Z-score 4.5–6, although they have low sequence homology (about 10%).

Since the catalytic activity of PG was inhibited by iodoacetamide, the catalytic center of PG was considered to be a cysteine residue (Yamaguchi et al. 2001). PG contains 11 Cys residues ( $\text{C}^{158}$ ,  $\text{C}^{167}$ ,  $\text{C}^{177}$ ,  $\text{C}^{195}$ ,  $\text{C}^{211}$ ,  $\text{C}^{212}$ ,  $\text{C}^{256}$ ,  $\text{C}^{261}$ ,  $\text{C}^{296}$ ,  $\text{C}^{307}$ , and  $\text{C}^{318}$ ). Considering both from the chemical shifts of  $\beta$ -carbons of cysteine residues and the calculated structure, four disulfide linkages can be assigned ( $\text{C}^{158}$ - $\text{C}^{167}$ ,  $\text{C}^{211}$ - $\text{C}^{307}$ ,  $\text{C}^{212}$ - $\text{C}^{261}$ , and  $\text{C}^{296}$ - $\text{C}^{318}$ ) but there are three free cysteine residues ( $\text{C}^{177}$ ,  $\text{C}^{195}$ , and  $\text{C}^{256}$ ) (Fig. 1C). The thiol group of  $\text{C}^{177}$  is exposed to the molecular surface, while those of  $\text{C}^{195}$  and  $\text{C}^{256}$  are buried. Further inspection of the DALI search revealed that the region encircled in Fig. 2A–E are similar so that the DALI search was applied again to the encircled region. The structures were well overlapped as are shown in Fig. 2F. Intriguingly, C177, H218 and D238 in PG are overlaid similarly with the catalytic triads in the DALI structural homologs including TGase3, factor XIII, FTG, thiol protease-like domain of *Pasteurella multacida* toxin (Fig. 2F) and thus these residues can be assigned to the catalytic triad in PG, but further biochemical studies are required.

Although PG catalyzes only protein-deamidation, transglutaminase (TG) catalyzes both protein-deamidation and protein cross-linking reactions. Therefore, it is intriguing to compare the structures of PG and TG from microbials to elucidate the difference in catalytic mechanism on the structural basis. A microbial TG (MTG) is comprised of 331 amino acids with a molecular mass of 37.9 kDa (Ando et al. 1989). MTG forms a single, compact domain (Kashiwagi et al. 2002), whereas other TGs form four domains (Noguchi et al. 2001; Yee et al. 1994). The



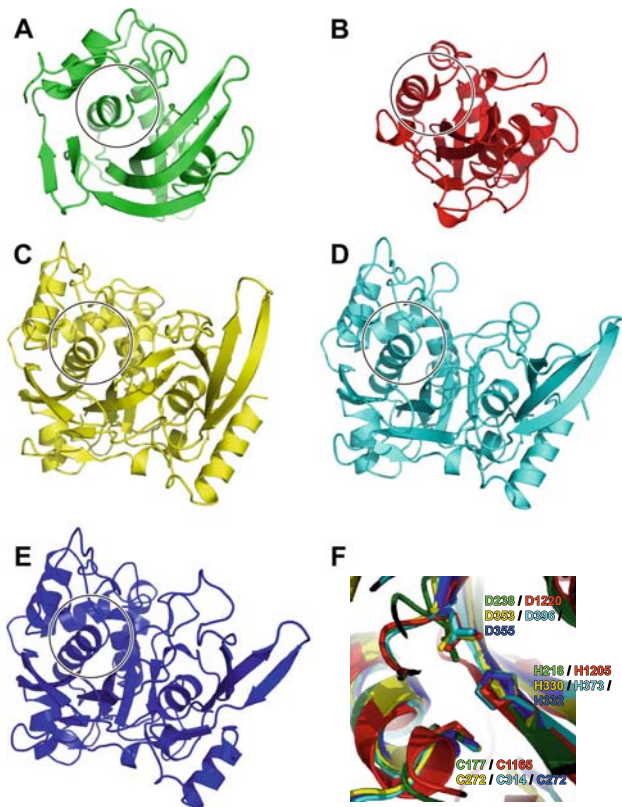


**Fig. 2** Structural homologues of PG. **A** PG, **B** thiol protease-like domain of *Pasteurella multacida* toxin (PDB: 2EBH), **C** TGase3 (PDB: 1L9 N), **D** factor XIII (PDB: 1GGY), and **E** fish TG (PDB: 1G0D). *Open circle* indicates the active site. **F** Superimposition of active site structures of PG and homologues, where the same color codes are used as in **A** to **E**. Catalytic triad residues (Cys–His–Asp) were presented in *stick model*

interaction between this surface and a substrate. In contrast, MTG has a deep cleft with a shallow negatively-charged pocket, where the catalytic cysteine is located. There are vestibules on the right and left sides of the deep cleft that presents a negatively-charged and hydrophobic surfaces, respectively (Fig. 3B). These vestibules would correspond to an acyl donor and an acyl acceptor binding sites (Kashiwagi et al. 2002). Other TGs similarly contain acyl donor and acceptor binding sites. The amido groups of the substrate glutamyl residue is hydrolyzed, the carboxylate group may be captured in the deep cleft and transferred to an acyl acceptor of a substrate protein.

In conclusion, the solution structure of PG was determined by NMR. The catalytic cysteine residue of PG was located at the deep negatively-charged pocket in the shallow cleft which prefers the glutamyl residue as a sole substrate. In contrast to MTG, PG has no binding site for an acyl donor protein, thus expels the resulting glutamyl residue from the negatively-charged pocket. This enables PG to have an efficient turnover of substrates.

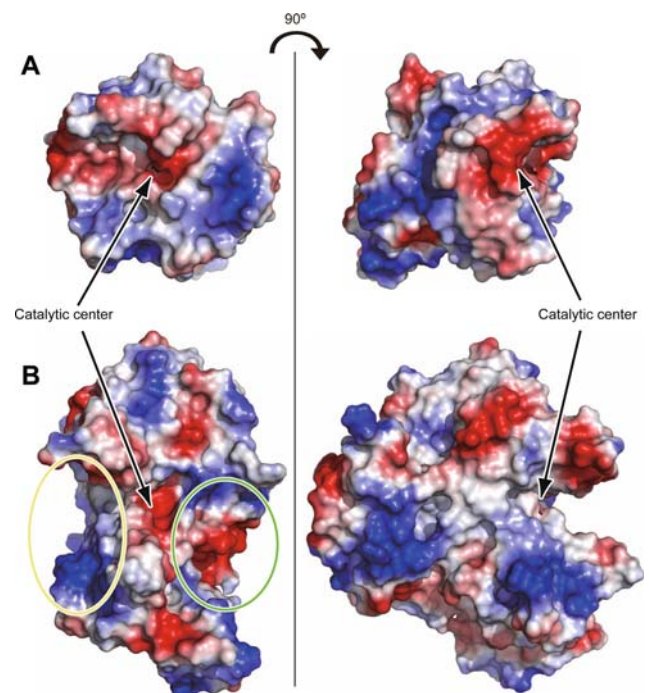


**Fig. 3** Electrostatic surface potential of PG (**A**) and MTG (**B**). Positive and negative charge densities are colored *red* and *blue*, respectively. The *arrow* shows the catalytic center in PG and MTG. **2** The structure is drawn using the program PyMOL with APBS tools (<http://www.pymol.org>). *Yellow* and *green* circles on the MTG structure indicated acyl donor (Gln residue) and acyl acceptor (primary amino group) binding sites, respectively

**Acknowledgments** We thank Hidehiko Wakabayashi and Noriki Nio of Institute of Life Sciences, Ajinomoto Co., Inc. for helpful discussion.

## References

- Ando H, Adachi M, Umeda K, Matsuura A, Nonaka M, Uchio R, Tanaka H, Motoki M (1989) Purification and characteristics of a novel transglutaminase derived from microorganisms. *Agric Biol Chem* 53:2613–2617
- Cornilescu G, Delaglio F, Bax A (1999) Protein backbone angle restraints from searching a database for chemical shift and sequence homology. *J Biomol NMR* 13:289–302
- Delaglio F, Grzesiek S, Vuister GW, Zhu G, Pfeifer J, Bax A (1995) NMRPipe: a multidimensional spectral processing system based on unix pipes. *J Biomol NMR* 6:277–293
- Goddard TD, Kneller DG (1997) SPARKY 3, University of California, San Francisco <http://www.cgl.ucsf.edu/home/sparky/>
- Herrmann T, Güntert P, Wüthrich K (2002) Protein NMR structure determination with automated NOE assignment using the new software CANDID and the torsion angle dynamics algorithm DYANA. *J Mol Biol* 319:209–227
- Holm L, Kaariainen S, Rosenstrom P, Schenkel A (2008) Searching protein structure databases with Dali Lite v.3. *Bioinformatics* 24:2780–2781
- Kashiwagi T, Yokoyama K, Ishikawa K, Ono K, Ejima D, Matsui H, Suzuki E (2002) Crystal structure of microbial transglutaminase

- from *Streptovorticillum mobaranse*. J Biol Chem 277:44252–44260
- Kikuchi Y, Itaya H, Data M, Matsui K, Wu L-F (2009) TatABC overexpression improves *Corynebacterium glutamicum* tat-dependent protein secretion. Appl Environ Microbiol 75:603–607
- Noguchi K, Ishikawa K, Yokoyama K, Ohtsuka T, Nio N, Suzuki E (2001) Crystal structure of red sea bream transglutaminase. J Biol Chem 276:12055–12059
- Shinagawa M, Shimba N, Mizukoshi T, Arashida N, Yamada N, Kikuchi Y, Suzuki E (2005) High expression with *Corynebacterium glutamicum* for nuclear magnetic resonance sample preparation. Anal Biochem 344:281–283
- Yamaguchi S, Jeenes DJ, Archer DB (2001) Protein-glutaminase from *Chryseobacterium proteolyticum*, an enzyme that deamidates glutaminyl residues in proteins. Eur J Biochem 268:1410–1421
- Yee VC, Pedersen LC, Le Trong I, Bishop PD, Stenkamp RE, Teller DC (1994) Three-dimensional structure of a transglutaminase: human blood coagulation factor XIII. Proc Natl Acad Sci 91:7296–7300